International Journal of Science and Research Archive

eISSN: 2582-8185

Cross Ref DOI: 10.30574/ijsra

Journal homepage: https://ijsra.net/

(RESEARCH ARTICLE)

Check for updates

Numerical study of the helicopter release problem considering rotor wake

Fabien Francois Frederick Costerg *

College of Aerospace Engineering, Nanjing University of Aeronautics and Astronautics, Nanjing, Jiangsu, 210016, China.

International Journal of Science and Research Archive, 2025, 15(02), 107-118

Publication history: Received on 23 March 2025; revised on 01 May 2025; accepted on 03 May 2025

Article DOI: https://doi.org/10.30574/ijsra.2025.15.2.1308

Abstract

This paper investigates the impact of the helicopter rotor wake on stores that could be launched from it. With use of unsteady flow solver and 6 degree of freedom equations, different cases of store release will be simulated. The model of helicopter used in this study is a simplified model of the UH-60A Black Hawk helicopter and the store is a simplified version of the Hellfire missile. Experimental validation of the solver and equations used will be conducted before investigating the release problem. Subsequent aerodynamic investigations were then conducted to quantify and analyze the path modification resulting from these perturbations: in hovering flight for different store launching thrust and in forward flight for different flight speeds. Results indicate a notable aerodynamic effect in the stores trajectory for hovering flight, changing its path prevision and altering its precision. For forward flight cases, simulations show lessen impact over the same missile paths.

Keywords: Helicopter; Computational Fluid Dynamics; Unsteady Flows; 6-Degrees-Of-Freedom

1. Introduction

For many years, helicopters have played a key role in military tactical operation on the battlefield. One of those missions among others is to carry and fire rockets from their board [1]. The rockets systems could be either free fall unguided rockets or guided rockets. After the release process and as it goes forward, the rockets could pass in the turbulent wake flow structure developed by the main rotor of the helicopter. Thus, its stability as well as its precision could be differently impacted by the turbulent airflow. It is then important to understand and quantify the impact that this phenomenon can have on the rocket.

Shanks and Ahmad [2] simulated the aerodynamics, missile dynamics, and plume of a finless missile breaking free from a wing in a transonic flow using a three-dimensional dynamic structured overset mesh approach. To investigate the impact of the missile and plume on the wing, a powered missile separation situation was taken into consideration in this study. Later, Cavallo et al. [3] performed numerical simulations of missile launch from a fighter aircraft and rocket stage separation. They employed a parallel moving mesh approach in conjunction with a three-dimensional unstructured mesh Navier-Stokes flow solver in their investigations. By carrying out a solution-adaptive mesh refinement, the accuracy of the solution was improved.

Related to helicopters, Taylor and Landgrebe [4] experimentally investigated the impact of a helicopter's main rotor on air-launched rockets using a model AH-1G helicopter engaged in low-speed forward flight. In their investigation, the wake flow created by the primary rotor was measured under various operational settings throughout the rockets' course. Also, numerical simulations of the trajectory of Penguin missiles fired from an SH2G helicopter were conducted by Wei and Gjestvang [5]. The rotor wake's generated interference velocity was calculated using a vortex wake model, and the fuselage airflow interference was estimated using a panel technique. Subsequently, the collected flow field data

* Corresponding author: Fabien Francois Frederick Costerg.

were transformed into the interference coefficients and integrated into a trajectory modeling system with six degrees of freedom.

More recently, Lee et al. [6] conducted a study for which a numerical technique based on unstructured meshes was devised to simulate air-launched rockets in free flight from a full helicopter configuration. An overset mesh approach was used to characterize the relative motion of the launched missiles, fuselage, main rotor, and tail rotor. To characterize the trajectory of air-launched rockets, six-degree-of-freedom dynamic equations of motion were combined with a flow solver. Calculations were performed for jet flow and rotor-fuselage interaction flow. It shows the temperature gradient along the helicopter fuselage, the flow of a rocket in a free flight and the perturbation caused by the rotor-wake. Zhou et al. [7] used numerical simulations to study the effects of the rotor wake on a free falling store and its impact on precision and release safety, revealing that the rotor's downwash flow can induce changes in the missile's attitude and trajectory immediately after release. For instance, research utilizing unsteady Computational Fluid Dynamics (CFD) coupled with six-degree-of-freedom (6-DOF) motion equations has demonstrated that the missile's pitch angle can increase under the influence of rotor downwash, leading to potential deviations from the intended flight path. Additionally, the determination of rotor wake boundary location has been shown to have a strong effect on rocket trajectory, emphasizing the need for accurate modeling of the rotor wake geometry to predict missile behavior effectively [8].

About UH-60A, Gong et al. [9] examined the downwash intake from the helicopter's rotor using the actuator disk model. A comparison was made between the downwash effects of a Sierra bullet and a Hydra70 rocket. It displayed the rocket's whole trajectory and range, and it was discovered that the downwash effect had a greater impact on the rocket than the bullet did. It did not, however, consider the effects of external wind, which skews the rotor wake and modifies the rocket's downwash effect, trajectory, and range.

The aim of this research is to quantify and analyze the impact the rotor wake can have on missile fired from it and for different launching cases. The CFD simulation will be performed on STAR CCM+ CFD software and will make use of the 6DOF equations model of the software to simulate the free movement of the missile in space.

2. UH-60A Simulation model

The helicopter used for the aim of this study is the UH-60A Black Hawk. For this study and as it is not judged to have enough impact, the tail rotor, the tail stabilizer and the wheels of the helicopter have been deleted from the model to obtain a lighter simulation file. The main rotor parameters of the helicopter are presented in Table 1:

Table 1 UH-60A rotor specification

Specification	Value
Nominal Rotor Speed	258 rpm (counterclockwise)
Number of blades	4
Rotor diameter	16,36 m
Tip Speed	221 m/s
Equivalent blade twist	-18 deg
Airfoil	SC 1095/SC1094 R8

The store used for the simulation is based on the AGM-116 Hellfire. The store is only present on the left-hand side of the helicopter for the simulation and only two are mounted on the launcher which is only composed of the support wing and the missile in order to simplify the simulation (Figure 1).

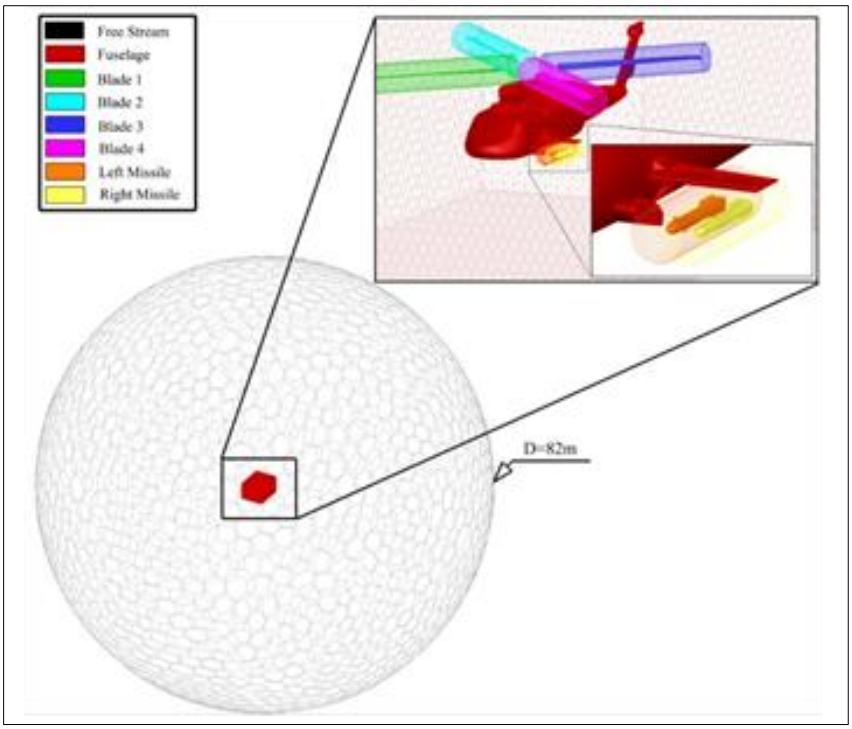

Figure 1 Helicopter CFD model geometry

3. Numerical method

3.1. Model equations and boundaries conditions

Into Star CCM+, the flow model used is an Unsteady Reynolds Averaged Navier-Stokes (URANS) which are derived of the Navier-Stokes equation and are composed of the continuity equation and the momentum equation respectfully. In this study, the flow is considered as perfect gas and incompressible. Then the set of 2 equations of the URANS are expressed as follows:

$$\frac{\partial \overline{u}_j}{\partial x_j} = 0 \qquad (1)$$

$$\frac{\partial \overline{u}_i}{\partial t} + \overline{u}_j \frac{\partial \overline{u}_i}{\partial x_j} = -\frac{1}{\rho}\frac{\partial \overline{p}}{\partial x_i} + \nu \frac{\partial^2 \overline{u}_i}{\partial x_j^2} - \frac{\partial \overline{u_i' u_j'}}{\partial x_j} \qquad (2)$$

To accommodate the model and take account of the unsteady part for the simulation, a turbulence model needs to be picked. The model chosen here is the Shear Stress Transport (SST) $k-\omega$ as introduced by Menter [10, 11]. It has the possibility to accommodate from a $k-\varepsilon$ model which has good performance in a free stream environment to a $k-\omega$ model who performs better for near wall case. The switch between the two models is operated with the addition of a blending function F_1. The SST $k-\omega$ set of equations calculating respectively the kinetic energy and the specific dissipation rate are thus as follows:

$$\frac{\partial k}{\partial t} + \overline{u}_j \frac{\partial k}{\partial x_j} = P_k - \beta^* k\omega + \frac{\partial}{\partial x_j}\left[(\nu + \sigma_k \nu_t)\frac{\partial k}{\partial x_j}\right] \qquad (3)$$

$$\frac{\partial \omega}{\partial t} + \overline{u}_j \frac{\partial \omega}{\partial x_j} = \alpha \frac{\omega}{k} P_k - \beta\omega^2 + \frac{\partial}{\partial x_j}\left[(\nu + \sigma_\omega \nu_t)\frac{\partial \omega}{\partial x_j}\right] + 2(1-F_1)\frac{\sigma_{\omega 2}}{\omega}\frac{\partial k}{\partial x_j}\frac{\partial \omega}{\partial x_j} \qquad (4)$$

For the boundary's conditions, the far field boundary will be considered as a free stream while for solid parts like the fuselage, the blades or the store, a wall slip tangency condition has been applied.

3.2. Unstructured overset meshes

For simulating multiple bodies in relative motions with each other, an overset mesh boundary conditions have been implemented [12, 13]. Thus, during the simulation, a search procedure will be conducted for each time step to find the donor cell to deactivate them and give the good condition to the cells judged active [14, 15]. The model is then completely meshed gradually from the body of the helicopter to the edges of the free stream with coarse mesh at the important calculation place and thinner for place who will not have much importance and charge computational resources. Figure 2 shows the mesh of the model from a plane section of Y axis normal. Ultimately, the model will be composed of 8 subdomains and a total of 9,078,503 mesh cells and 28,879,975 vertices which require a lot of computational resources.

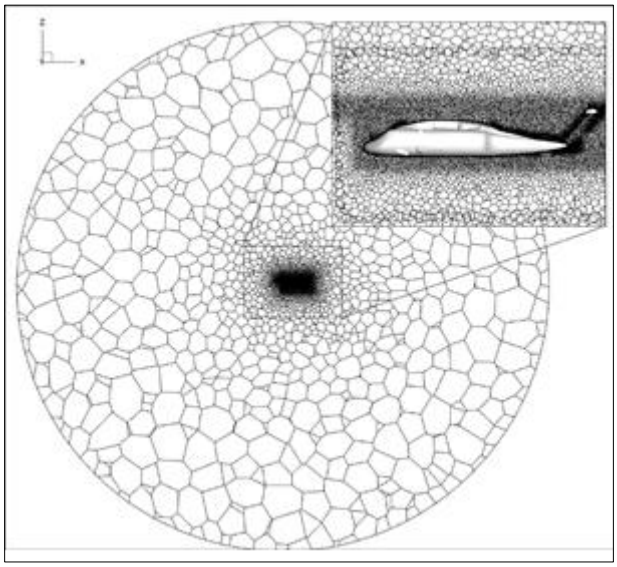

Figure 2 Meshing of the domain

3.3. Temporal and Spatial discretization

For the spatial discretization, the Finite Volume Method (FVM) is used. This method involves dividing the computational domain into a grid composed of polyhedral cells in this case, which offers flexibility in capturing complex geometries. The overset grid approach, used in this work, further enhances this by allowing overlapping grids to handle relative motion between components, such as rotating blades and stationary fuselage, through interpolation across grid interfaces.

For the temporal discretization, an Implicit Unsteady solver has been chosen. The method used here is the Backward Euler Method (1st order) [16]. The time step used in the simulation corresponds then to an azimuthal angle ψ of 2° for each time step.

4. Results and Discussions

Multiple cases will be run in this work ranging from verification and validation to store release in hovering flight as well as for forward flight. All the computation has been conducted on a computer equipped with Intel Xeon CPU of 40 cores and 40 threads as well as 116 GB of RAM. Even if the computational power present is interesting, each simulation would still take approximately 78hrs to complete.

4.1. Validation of the 6DOF equations and URANS solver

To validate the 6DOF equations and the unstructured overset grid method, the EGLIN wing store model has been simulated and compared to its experimental data. This model consists of a delta wing with a pylon mounted on it and free drop a cylindrical store from it (Figure 3). The store will be pushed downward by two ejectors placed on the pylon with a stroke length of 100mm [17].

The simulation will last 1s and the position of the store will be saved each 0.1s. Figure 4 shows the evolution of the store for each 0.1s time interval. It is possible to see that the store has a clear free fall movement which is lightly influenced by the presence of the fins at the back of it.

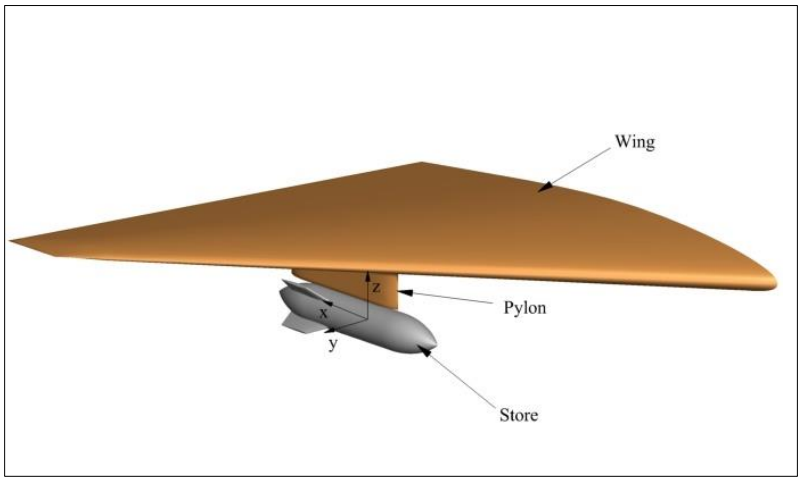

Figure 2 EGLIN wing/store separation model

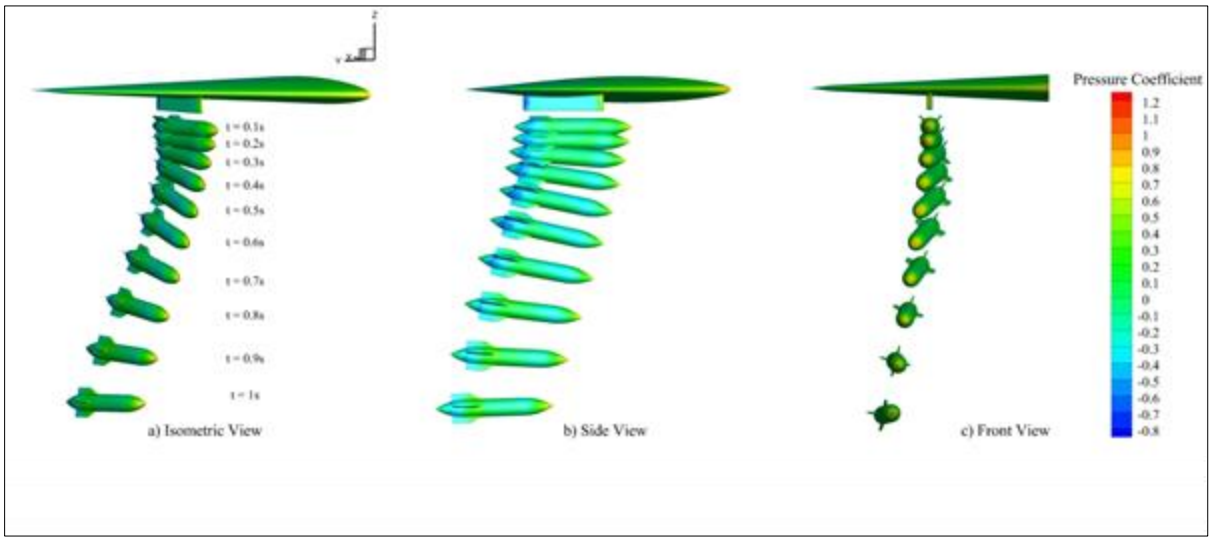

Figure 4 Store separation at every 0.1s time interval

Figure 5 then shows the comparison of the Center of Gravity (CG) position and velocity in function of time with the experimental data obtained by Heim [18]. The figures show a good correlation between the CFD simulation and the experimental work. Indeed, the path of the store follows with an acceptable error the experimental data and thus shows the capability of the solver to represent free fall and 6DOF movement.

4.2. Store release in hovering flight

In hovering flight configuration, the helicopter generates a high turbulent rotor wake flowing downward and comprise in the rotor disk area as seen on Figure 6. This wake is composed of highly turbulent air mostly due to Tip Vortices (TV) and Blade Vortex Interaction (BVI) [19].

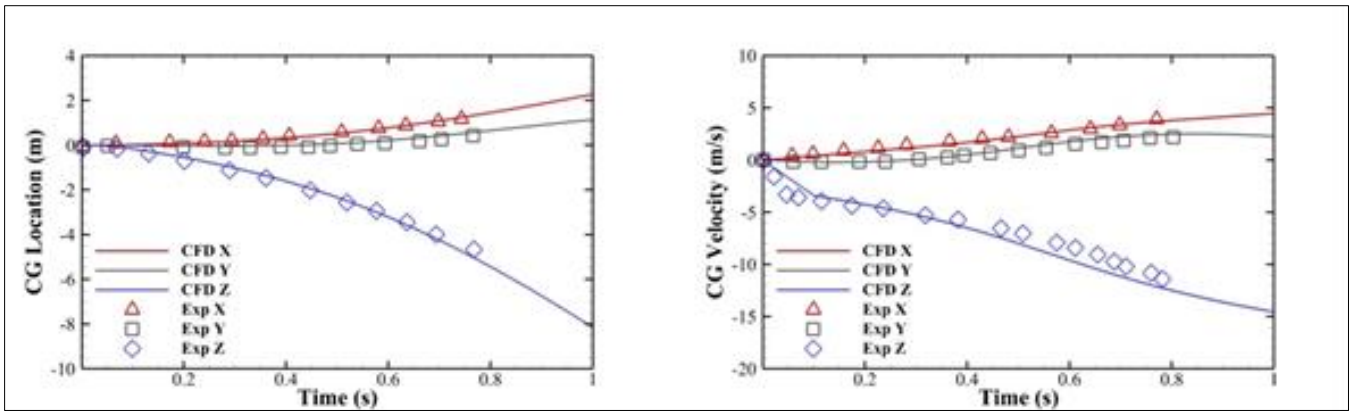

Figure 5 CG displacement and velocity compared with experimental value

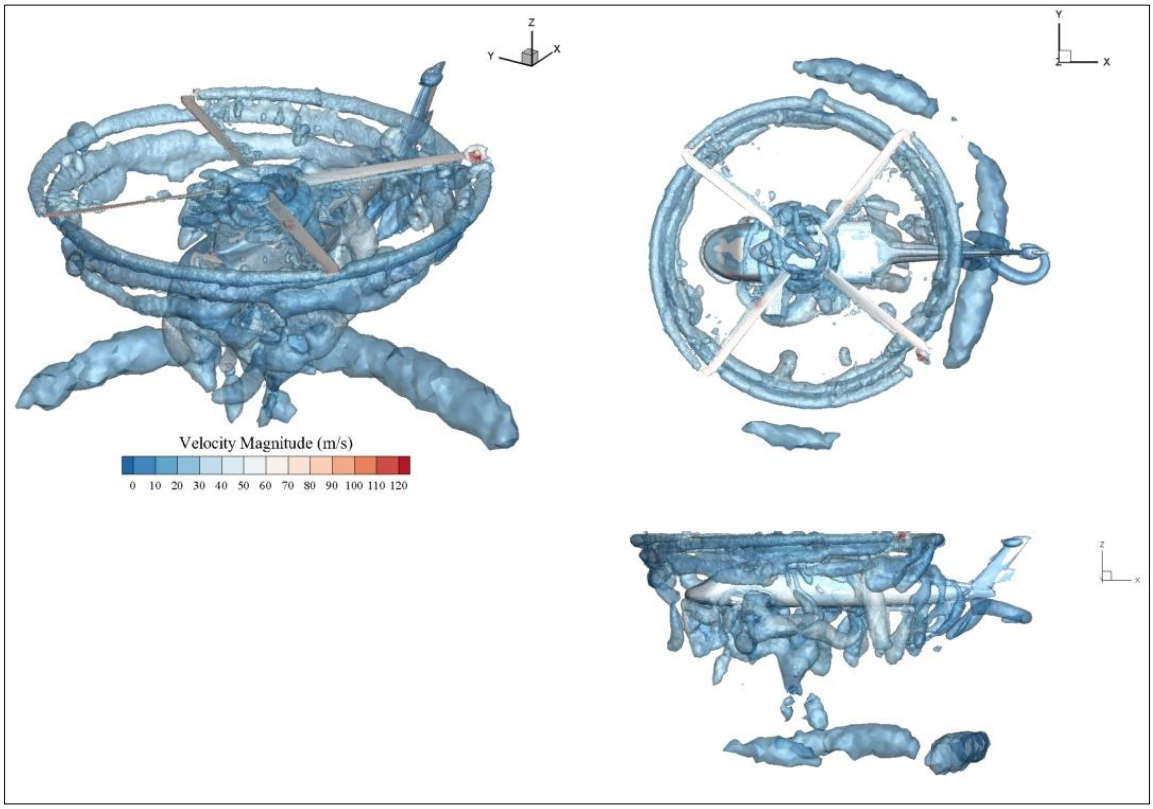

Figure 6 Hovering air velocity magnitude plotted for a Q-criterion vorticity of 50

In this disposition, the store release will be tested for 3 different thrusts of 13600N/7174N/5180N. Those thrust values have been chosen to be close to the real value of Hellfire's thrust and other type of store as in the study of Lee et al. [6].The simulation will then run for 3 rotor rotation in order to the airflow to stabilize and thus the store will be launched in a free 6DOF movement with a constant unidirectional thrust condition situated on the nozzle of the rocket on its X local axis (Figure 7).

Figure 8 shows the evolution of the store CG position in all different axis as a function of the simulation time from the moment it gets released. In Figure 8-a, the Longitudinal (X) axis movement shows a nominal trajectory in a case of constant acceleration and thus linear speed. That means the air doesn't have any significant impact on the store longitudinal trajectory. For the horizontal displacement (Y axis), Figure 8-b shows a movement of the store to its right. This could be explained with the presence of stabilizers at the front and the back of the store who can be impacted differently by the turbulent air illustrated before.

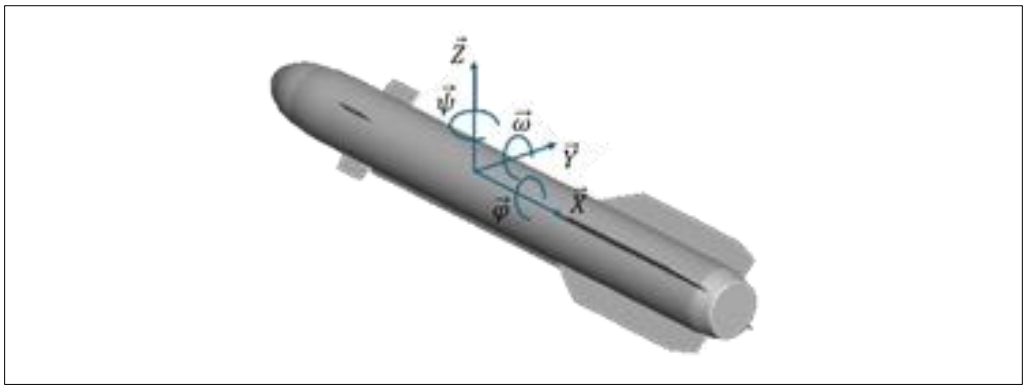

Figure 7 CFD model of the store and its coordinates system

For the vertical displacement (Z axis), Figure 8-c doesn't show any reliable modification in the store path. The drop-down trajectory of the store indicates that the dropping speed could be constant and that the wake airflow doesn't have a significant impact on it. One case differs from the others and sees its trajectory change from a drop-down trajectory to a slight positive climb one.

At the same time, the store rotation is an important parameter to better understand the impact of the rotor wake flow.

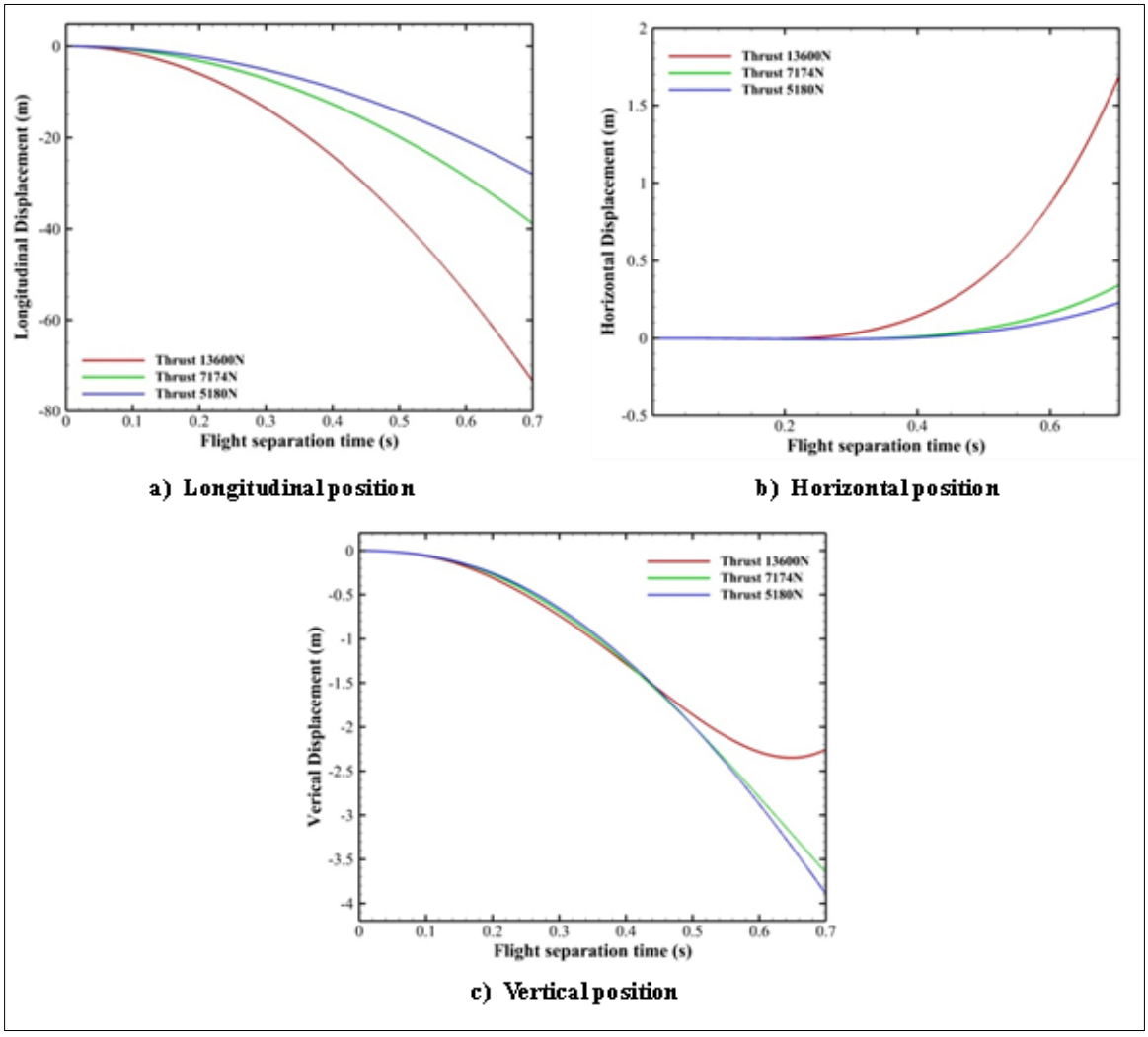

Figure 8 Comparison of the store CG position for different launching thrust in hovering flight a) Longitudinal position b) Horizontal position c) Vertical position

For the Roll angle (around X axis), Figure 9-a shows the difference of angle change with the difference of thrust. Indeed, for low thrust, as the store spends more time in the wake flow, the turbulent downward flow could impact its trajectory by interacting with the front and back lateral fins. Figure 9-b shows an increase in the maximum Pitch (around Y axis) angle that the store takes during the time it interacts with the rotor wake. Thus, for a store released with a thrust of 5185N, the total maximum pitch angle observed will be of -4° while, for one released at a thrust of 13600N, the maximum angle will then be of -2°. This change in pitch angle shows the impact of rotor wake as it changes adequately with the decrease in the launch thrust.

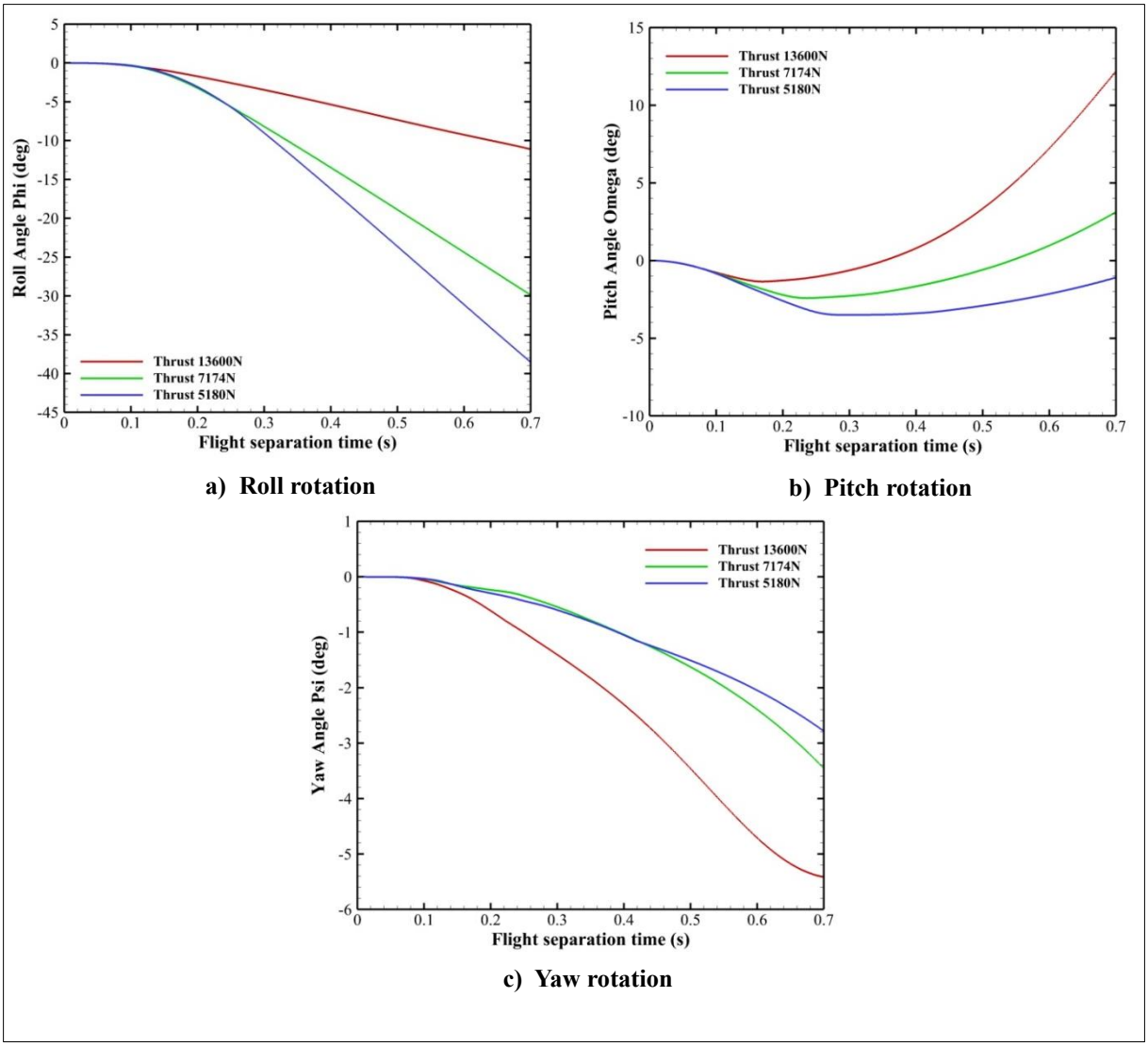

Figure 9 Comparison of the store rotation for different launching thrust in hovering flight a) Roll rotation b) Pitch rotation c) Yaw rotation

Then, the Yaw rotation (around Z axis), pictured in Figure 9-c shows a higher impact for the highest thrust store while the lowest thrust one will get less impacted with a difference of more the 2°.

4.3. Store release in forward flight

In the case of a forward flight configuration, the helicopter's rotor wake flow will interact with the incoming airflow and thus move along the body of the helicopter as seen in Figure 10. For these cases, the BVI will be more important while the TV will be stronger but got pushed backward by the incoming air flow [20].

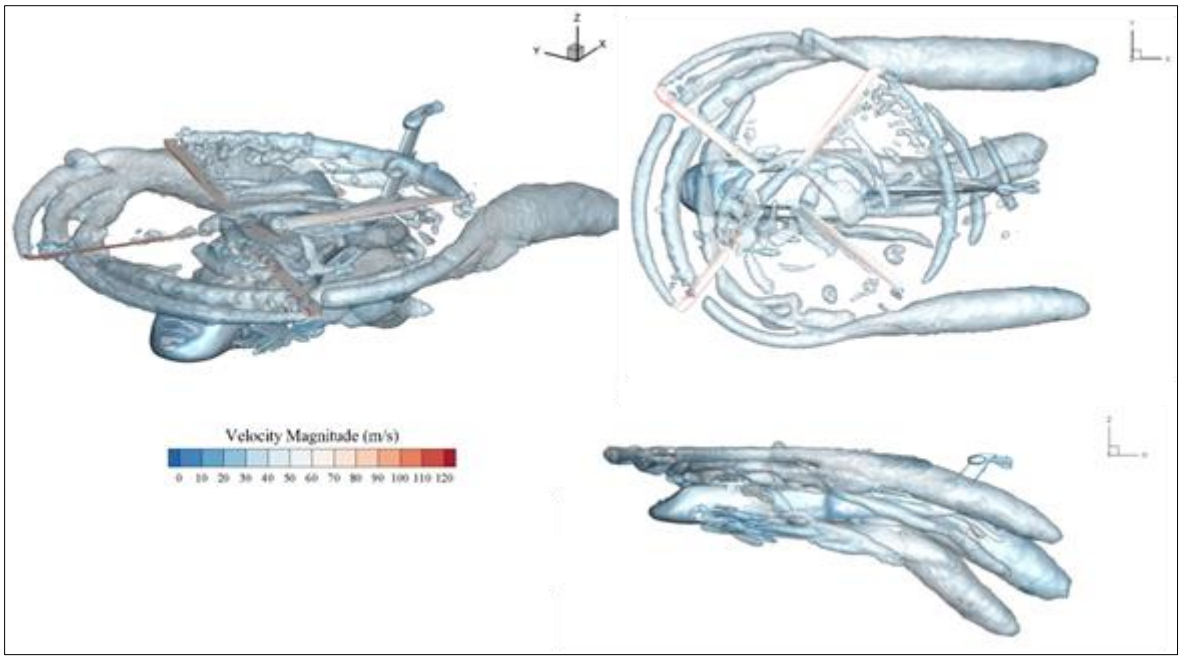

Figure 10 Forward flight speed of 100kph air velocity magnitude plotted for a Q-criterion vorticity of 50

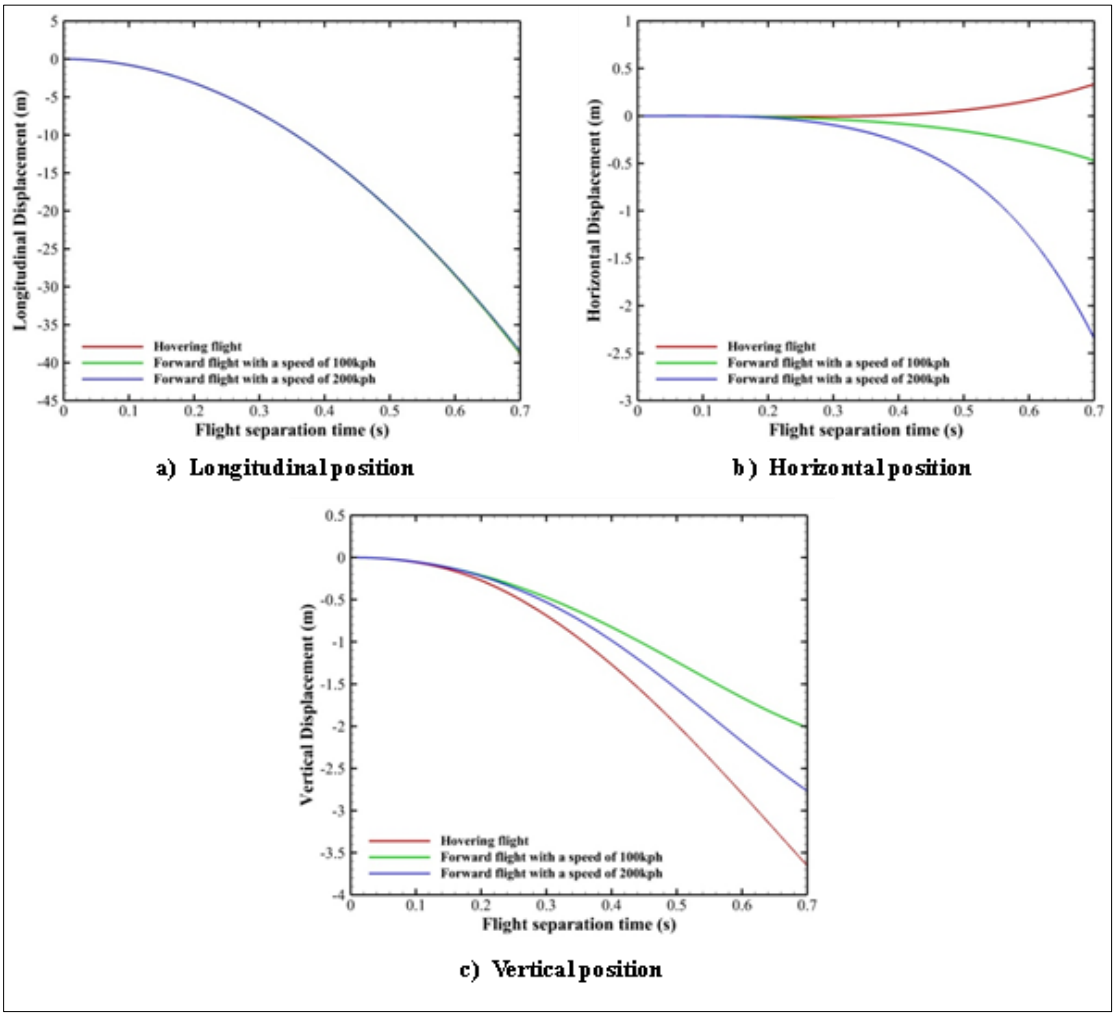

Figure 11 Comparison of the store CG position for different helicopter forward speed a) Longitudinal position b) Horizontal position c) Vertical position

For this part, the store release will be tested for the same launching thrust of 7174N and for 2 different forward flight speeds of 100 kilometer per hour (kph) and 200 kph. The helicopter velocity is in a good range between a velocity of 0 and the maximum velocity of 275 kph that the UH-60 could travel. Thus, the simulation will also run for 3 rotor rotation in order for the airflow to stabilize and thus the store will be launched accordingly with the hovering flight cases. To interpret the values recorded, they will be compared with the hovering flight case at the same store launching thrust.

In Figure 11-a, the longitudinal movement of the CG as a function of the simulation time shows a nominal curve characteristic of a movement in constant acceleration and linear speed implying no real effect from the incoming air or the rotor wake. Figure 11-b shows the horizontal displacement of the CG, in comparison with the hovering case, the store has more tendency to go to its left side. This movement could be explained by the presence of the fins on the front and the back of the rocket that interacts with the incoming airflow as the rotor wake is less present in this area. In Figure 11-c, the vertical movement, point that the drop rate of the missile is decreasing for the store that are not launched in hover with a difference of almost 1m between each other at the end of the simulation. The difference shows the least impact of the rotor wake on the store for the forward flight cases as its presence is highly diminishing. Another explanation can come from the fact that the air coming forward can interact with the missile's fins to generate residentials lift that lowers this drop rate.

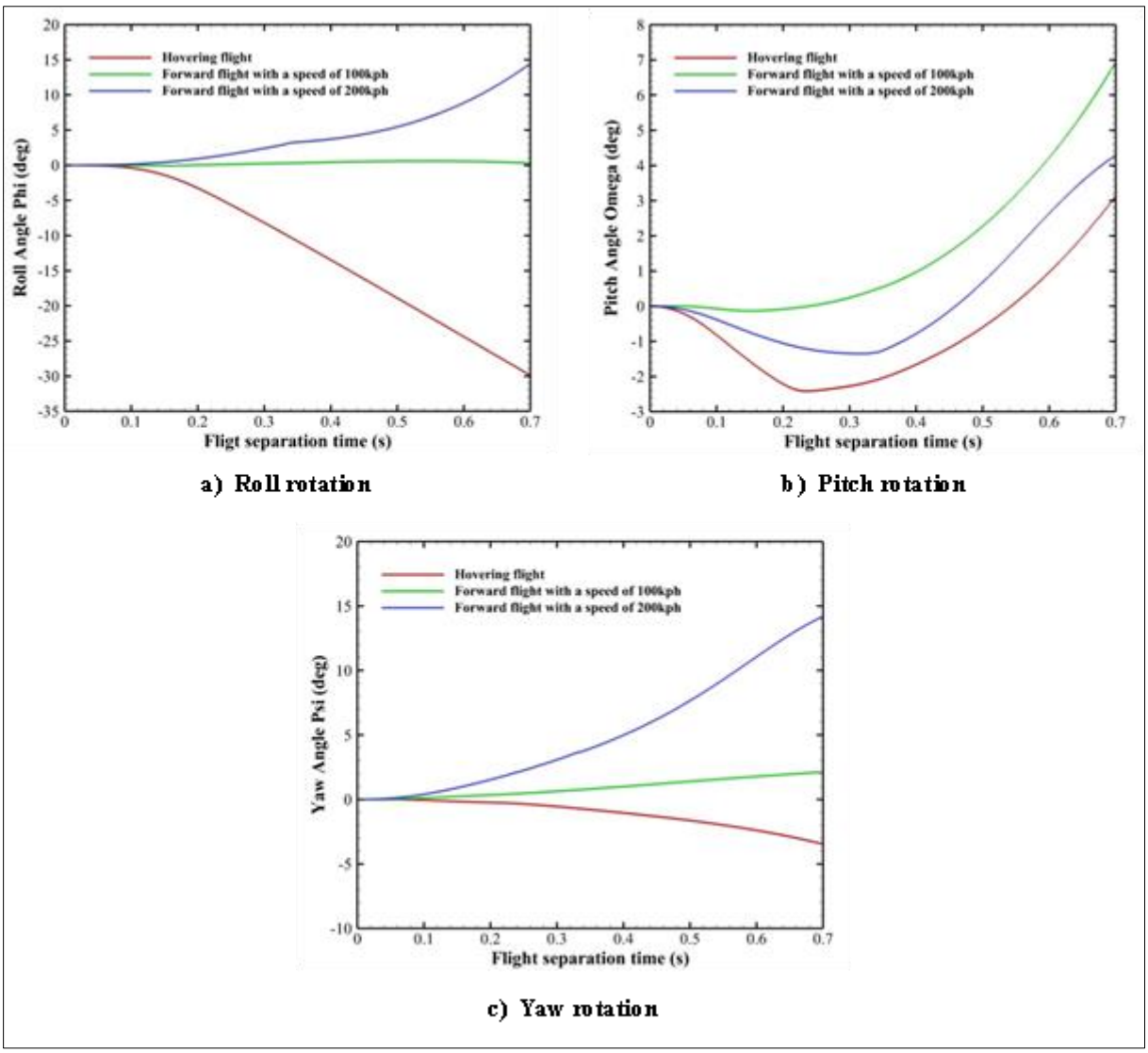

Figure 12 Comparison of the store rotation for different helicopter forward flight speed a) Roll rotation b) Pitch rotation c) Yaw rotation

For the angular rotation, Figure 12 shows that the roll, pitch and yaw evolution follow the same patterns between each of them: when the helicopter fly at a cruising speed of 100 kph, the store show a nominal trajectory with no significant

change in its rotation except for the pitching angle which enlighten a slight pitch-up of the nose of the store at an important rate during the launching. Anyway, for the forward case flight at 200 kph, the rocket acts at the opposite of the hovering case. This difference of behavior shows that some parameters have influenced the missile and must be related to the absence of rotor wake acting on it.

Nomenclature

- URANS = Unsteady Reynolds Averaged Navier-Stokes
- CFD = Computational Fluid Dynamics
- CG = Center of Gravity
- 6DOF = 6-degree-of-freedom
- TV = Tip Vortice
- BVI = Blade Vortex Interaction
- F_1 = SST $k-\omega$ blending function
- k = Turbulent kinetic energy
- ω = Specific dissipation rate
- ν_t = Turbulent Eddy viscosity
- $\bar{p}$ = Mean pressure
- T = Time
- $\overline{u_i}$ = Mean component of the fluid velocity
- x_i, x_j = Spatial Coordinates

5. Conclusion

This paper presents an extensive simulation of unsteady flow fields around a helicopter configuration to determine the impact of the rotor wake on a store that could have been launched from it in different flight conditions. For this purpose, an unsteady RANS flow solver has been used as well as a six degree of freedom motions equations inside of STAR CCM+ CFD simulation software to simulate the store flight in space.

To validate the solver and the 6DOF equations capability, the free fall motions of a store has been compared with experimental data and showed no important divergence on the store path. After it, a comprehensive aerodynamic analysis of the rotor wake impact was conducted and showed considerable impact in function of the flight conditions. Indeed, for hovering flight, as the store passes through the turbulent wake created by the rotor rotation, the trajectory is subsequently modified. Although, the thrust of the released store is also an important parameter to acknowledge as it can also impact its path as it spends more or less time through the turbulent air. Contrarily, for a forward flight, the path seems less impacted by the wake as the flow is directed along the helicopter body and thus has less possibility to interact with the store.

However, the model and simulation performed here still presents certain limitations. The current model uses store geometry that don't have been extensively tested and thus could be subject to miss conception and impacting the simulation. This study only used stores on the left side of the helicopter in order to facilitate the computation. Since the tip vortices at the rotor's blades don't have the same intensity for the advancing blade and the retracting blade, it could be interesting to investigate and experiment a release from both sides simultaneously.

References

[1] Petrescu RV, Aversa R, Akash B, Corchado J, Berto F, Apicella A, Petrescu FI. About Helicopters. Journal of Aircraft and Spacecraft Technology. 2017;1(3):204-223.

[2] Shanks S, Ahmad J. Aerodynamics of powered missile separation from a wing. 22nd Fluid Dynamics, Plasma Dynamics and Lasers Conference, Honolulu, USA, 1991.

[3] Cavallo P, Sinha N, Feldman G. Parallel Unstructured Mesh Adaptation for Transient Moving Body and Aeropropulsive Applications. 42nd AIAA Aerospace Sciences Meeting and Exhibit, Reno, USA, 2004.

[4] Taylor RB, Landgrebe AJ. Investigation of the Airflow at Rocket Trajectory and Wind Sensor Locations of a Model Helicopter Simulating Low Speed Flight. 1979.

[5] Wei FS, Gjestvang J. Store separation analysis of the Penguin missile from the SH-2G helicopter. 39th Aerospace Sciences Meeting and Exhibit, Reno, USA, 2001.

[6] Lee BS, Choi JH, Kwon OJ. Numerical Simulation of Free-Flight Rockets Air-Launched From a Helicopter. Journal of Aircraft. 2011;48(5):1766-1775.

[7] Zhou WY, Yang GC, Gao X, Zhou XY, Zhou BX. Numerical Simulation of Missile Air-Launched Dynamic Process Under Downwash Flow of Helicopter Rotor. 33rd Congress of the International Council of the Aeronautical Sciences, Stockholm, Sweden, 2022.

[8] Kapulu O, Tekinalp O. Main Rotor Downwash Effect on Separation Characteristics of External Stores. AIAA Atmospheric Flight Mechanics Conference, Grapevine, USA, 2017.

[9] Gong H, Kwak E, Lee S, Park JS. Prediction of Trajectories of Projectiles Launched from Helicopters. Journal of the Korean Society for Aeronautical & Space Sciences. 2014;42(3):213-220.

[10] Menter FR. Improved Two-Equation k-omega Turbulence Models for Aerodynamic Flows. 1992.

[11] Menter FR. Two-Equation Eddy-Viscosity Turbulence Models for Engineering Applications. AIAA Journal. 1994;32(8):1598-1605.

[12] Meakin RL. A new method for establishing intergrid communication among systems of overset grids. 10th Computational Fluid Dynamics Conference, Honolulu, USA, 1991.

[13] Steger JL, Dougherty FC, Benek JA. A Chimera Grid Scheme. 1983.

[14] Roget B, Sitaraman J. Robustness and Accuracy of Donor Search Algorithms on Partitioned Unstructured Grids. 10th Symposium on Overset Composite Grids and Solution Technology, Moffet Field, USA, 2010.

[15] Bonet J, Peraire J. An alternating digital tree (ADT) algorithm for 3D geometric searching and intersection problems. International Journal for Numerical Methods in Engineering. 1991;31(1):1-17.

[16] Cox C, Liang CC, Plesniak MW. A flux reconstruction solver for unsteady incompressible viscous flow using artificial compressibility with implicit dual time stepping. 54th Aerospace Sciences Meeting, AIAA SciTech, San DIego, USA, 2016.

[17] Panagiotopoulos EE, Kyparissis SD. CFD Transonic Store Separation Trajectory Predictions with Comparison to Wind Tunnel Investigations. International Journal of Engineering. 2010;3(6):538-553.

[18] Heim ER. CFD wing/pylon/finned store mutual interference wind tunnel experiment. 1991.

[19] Landgrebe AJ. The Wake Geometry of a Hovering Helicopter Rotor and Its Influence on Rotor Performance. Journal of American Helicopter Society. 1972;17(4):3-15.

[20] Chaderjian NM. Navier-Stokes Simulation of UH-60A Rotor/Wake Interaction Using Adaptive Mesh Refinement. AHS International Annual Forum & Technology Display, Fort Worth, USA, 2017.

Authors Short Biography

Fabien François Frederic Costerg, born in May 2000, is a student pursuing a double master's degree in mechanical and aerospace engineering at the Nanjing University of Aeronautics and Astronautics (NUAA) and the Ecole Nationale d'Ingénieurs de Metz (ENIM). His master's thesis focused on the effect of the helicopter rotor wake on released store.